Journal of Atmospheric and Terrestrial Physics, Vol. 53, No. 8, pp. 773–779, 1991.
Printed in Great Britain.

0021-9169/91 $3.00+ .00
Pergamon Press plc

Multiple beam observations of mid-latitude ionospheric disturbances by the MU radar

TOMOYUKI TAKAMI,* SHOICHIRO FUKAO,* W. L. OLIVER,† SUSUMU KATO,* TOSHITAKA TSUDA,* TORU SATO,‡ MANABU D. YAMANAKA,* MAMORU YAMAMOTO* and TAKUJI NAKAMURA*

*Radio Atmospheric Science Center, Kyoto University, Uji, Kyoto 611, Japan; †Department of Electrical, Computer and Systems Engineering, Boston University, Boston, MA 02215, U.S.A.; ‡Department of Electrical Engineering, Kyoto University, Yoshida, Kyoto 606, Japan

(*Received in final form* 11 *February* 1991)

Abstract—The pulse-to-pulse beam steerability of the MU radar of Kyoto University enables us to observe multiple beam positions simultaneously. Based on 560 h of this type of data, we present two typical patterns of mid-latitude ionospheric disturbances and their horizontal traveling characteristics. Wavy structures have not been found in large-scale disturbances. Isolated disturbances travel primarily southward (equatorward) in disturbed conditions, while no preferred direction is observed in quiet conditions.

1. INTRODUCTION

The Middle and Upper atmosphere (MU) radar of Kyoto University at Shigaraki, Japan (35°N, 136°E) is the most recent of the large atmospheric radars capable of detecting incoherent scatter (IS) from the free electrons in the ionosphere. IS observations of the *F*-region with the MU radar began in December 1985, and they have been performed periodically since September 1986 at monthly intervals. Based on the data obtained by MU radar IS observations, several studies of ionospheric *F*-region disturbances at mid-latitudes have been carried out. OLIVER *et al.* (1988) have discussed the disturbance due to atmospheric gravity waves during the large geomagnetic storm of 6–8 February 1986. SARYO *et al.* (1989) have reported measurements of the electron density midday bite-out phenomena. REDDY *et al.* (1990) have discussed the disturbance due to the electric field associated with the intense substorm of 20–21 January 1989.

The greatest advantage of the MU radar IS measurement is the capability to observe in multiple directions simultaneously by pulse-to-pulse beam steerability. This observational technique is very useful for the study of ionospheric disturbances because we can clearly detect disturbances by observing the difference between signal powers in the different beam directions.

In this paper we mainly describe details of the MU radar multiple beam observations and some examples of the data analyses of two typical patterns (traveling and non-traveling) of mid-latitude ionospheric disturbances. We shall present preliminary results of the horizontal traveling characteristics of 47 traveling ionospheric disturbances found in the mid-latitude *F*-region with the MU radar multiple beam IS observations during more than 560 h.

2. MULTIPLE BEAM OBSERVATIONS

A general description of the MU radar system has been given by FUKAO *et al.* (1985a, b), and SATO *et al.* (1989) discussed its sensitivity for IS measurements. A summary of the MU radar system parameters is shown in Table 1. Here we present only a detailed description concerning multiple beam observations.

The MU radar is a monostatic pulse radar with an active phased-array system, which is composed of 475 antenna array elements and an identical number of transmitter–receiver (TR) modules. Each array element is connected to a separate low-power TR module which can be driven coherently with low-level pulses. All phase shifting and signal division/recombination is carried out at a low power (about 2.2 kW). Therefore the antenna can be phased to observe in different directions on a pulse-by-pulse basis, which we call the multiple beam mode of observation. By this technique we can observe in multiple directions simultaneously.

Table 2 shows the main observational parameters normally used for the MU radar multiple beam observations of the IS power profile, from which the electron density profile can be estimated. The antenna beam was sequentially steered to four oblique directions (magnetic north, east, west and south), at a

Table 1. Basic parameters of the MU radar (OLIVER *et al.*, 1988)

Parameter	Value
Location	Shigaraki, Shiga, Japan (34.85°N, 136.10°E)
Geomagnetic parameters (300 m altitude) (IGRF 1985)	Field strength: 0.0402 mT Declination: 5.7°W Dip angle: 48.3° Dip latitude: 29.3°
Operational frequency	46.5 MHz
Antenna	Circular array of 475 crossed Yagis
Aperture	8330 m^2
Steerability	0-30° off-zenith, 5° azimuth steps
Partitioning	25 groups of 19 elements each, each separately driveable
Transmitter	475 solid-state amplifiers (one for each antenna element), 2.4 kW peak (120 W average) power each
Peak power	1 MW maximum
Average power	50 kW maximum
Pulse length	1–512 μs
IPP	0.4–65 ms

Table 2. Observational parameters of the MU radar multiple beam observation

Parameter	Value
Antenna beam direction	Geomagnetic north, east, west and south at 20° zenith angle
Pulse width	512 μs or 256 μs
IPP	10300 μs
Observed heights	200–600 km
Height resolution	~75 km
Incoherent integration	240 s^{-1}

zenith angle of 20°. With this configuration the distance between scattering volumes in each beam position is 200–300 km at typical *F*-region altitudes as shown in Fig. 1. The signal power of an oblique beam is different from that of another beam if the electron density is not homogeneous in space. In order to detect the actual difference ΔP between signal powers in two different beams, the random statistical fluctuation δP of the signal power must be sufficiently less than ΔP, that is, $\Delta P/P \gg \delta P/P$, where P is the total signal power. We have

$$\frac{\delta P}{P} \sim \frac{1}{\sqrt{M}}\left(1+\frac{1}{SNR}\right) \qquad (1)$$

where SNR denotes the signal-to-noise ratio and M is the number of incoherent integrations. In the case of a time resolution of 5 or 6 min, the number of incoherent integrations is approximately 10,000 when we use the parameters shown in Table 2. Then $\delta P/P \sim 0.02$ if the signal-to-noise ratio is greater than unity. Therefore, when $\Delta P/P \gg 0.02$, we can observe the actual difference between signal powers in different oblique beams by these multiple beam observations.

It is important for the MU radar multiple beam observations to make the signal-to-noise ratio greater than unity. In order to maximize the signal-to-noise ratio, we usually use a pulse width of 512 μs, which is the largest width available for the MU radar system.

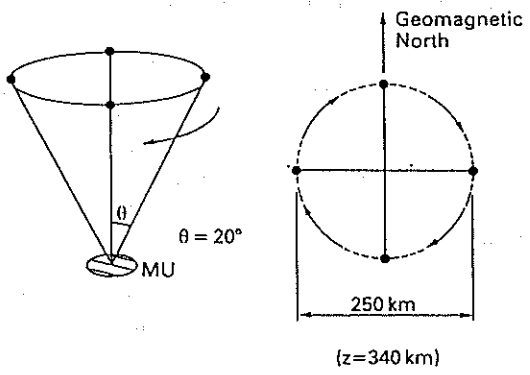

Fig. 1. Schematic diagrams of the beam directions used in the MU radar multiple beam observations. The antenna beam is sequentially steered to four oblique directions (magnetic north, east, west and south), at a zenith angle of 20°. With this configuration the distance between scattering volumes in each beam position is 200–300 km at the *F*-region altitudes.

For long-pulse power profile measurement, the signal-to-noise ratio becomes greater than unity over a considerable range around the $F2$ peak altitude, so that it is practicable to perform multiple beam observations of the ionospheric F-region.

3. IONOSPHERIC DISTURBANCES

We present here typical features of ionospheric disturbances obtained by the multiple beam observations with the MU radar. Disturbances observed are classified into the following two types: type-A is defined by a non-zero phase difference between signals detected in different oblique beams, and type-B is defined by zero phase difference between them.

3.1. *Traveling disturbances*

Figure 2 shows the time variation of signal powers obtained by the MU radar multiple beam observation performed after midnight on 16 March 1989. We have an example of the type-A disturbance in these data. From 0130 to 0230 LT, an ionospheric disturbance was observed in all the oblique beams as variations of the signal power. Variations of the signal power correspond to variations of the electron density in the F-region. It is found that the signal power maximum in the geomagnetically north oblique beam appeared earlier than that in the south beam maximum. There is almost no time lag between the signal power maxima in the east and west oblique beam. These features indicate that this disturbance traveled almost directly from north to south. The travel speed of the disturbance is determined from the phase difference between signal power variations in different oblique beams. In this case, the speed can be estimated as approximately 150 m/s. The time lag between the signal power maxima of the north and south beams increased with altitude. This feature suggests that this

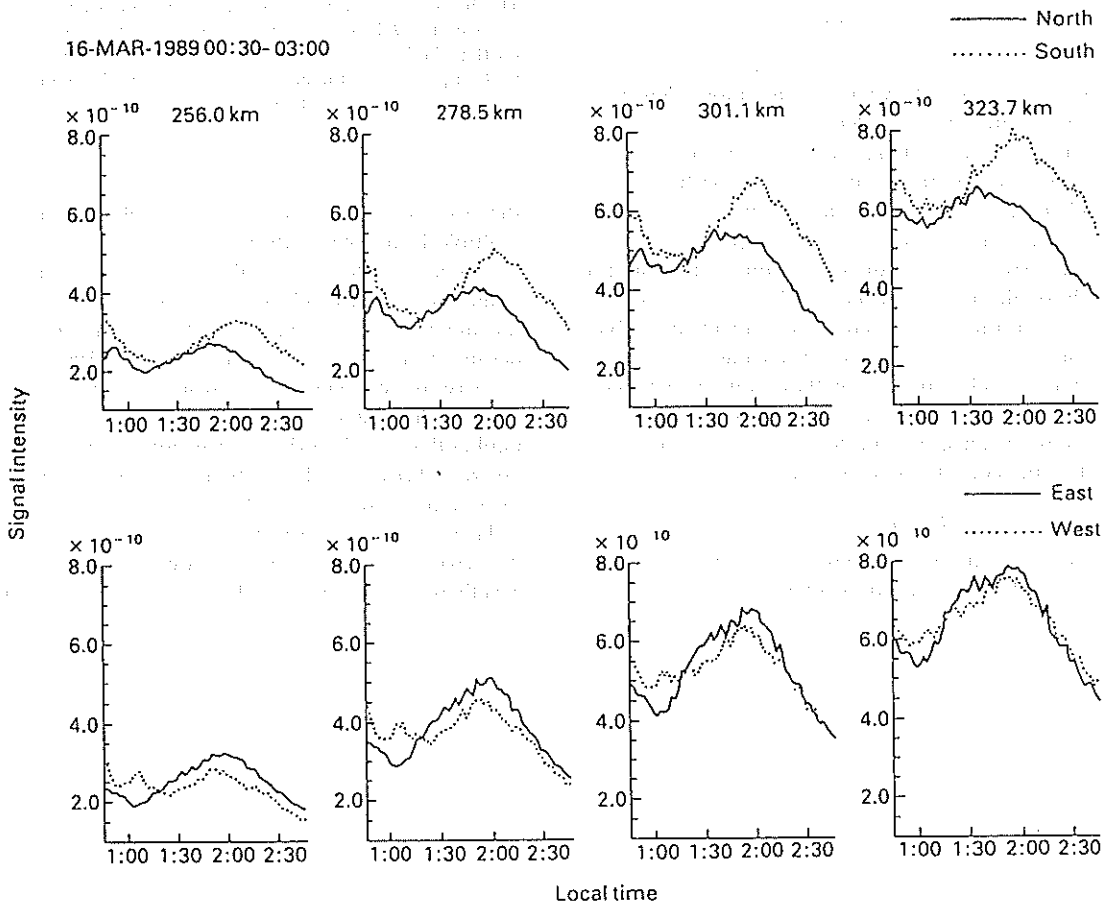

Fig. 2. Temporal variations of signal powers obtained by the MU radar multiple beam observation performed after midnight on 16 March 1989. The top four plots show the data in the north (solid line) and south oblique (dotted line) beams at heights of 256, 278, 301 and 323 km. The bottom four plots show the data in the east (solid line) and west oblique (dotted line) beams at the same height as the plots above.

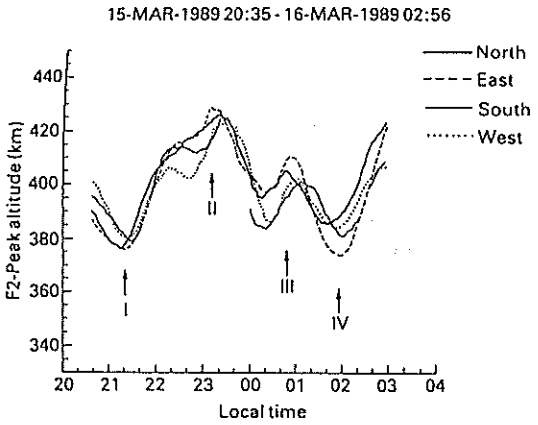

Fig. 3. Temporal variations of the $F2$ peak altitude obtained by MU radar multiple beam observations performed during the night of 15–16 March 1989. The thick solid line is for the north oblique beam, the thick dotted line for the east beam, the thin solid line for the south beam and the thin dotted line for the west beam. I, II, III and IV show ionospheric disturbances.

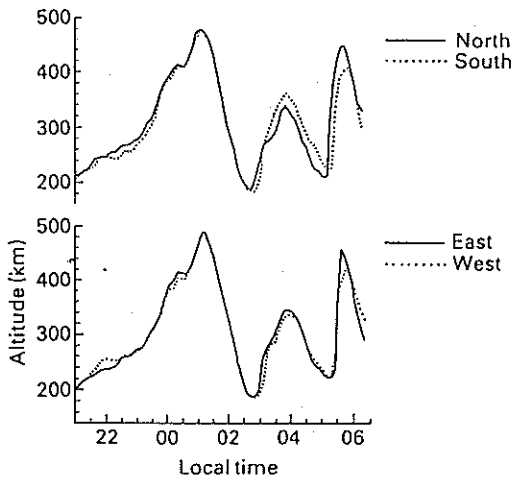

Fig. 5. Temporal variations of the height z_L at which the electron density is 6×10^4 cm^{-3}, obtained by the multiple beam observation during the night of 20–21 January 1989. The height z_L corresponds to the minimum virtual height ($h'F$) of the F-layer. The top plot shows the data in the north (solid line) and south oblique (dotted line) beams. The bottom plot shows the data in the east (solid line) and west oblique (dotted line) beams.

disturbance was traveling at an almost constant velocity at an altitude of 200–400 km.

Figure 3 shows temporal variations of the $F2$ peak altitude during the night of 15–16 March 1989. Ionospheric disturbances appeared as variations of the $F2$ peak altitude in these data. The passage of type-A disturbances was found at four different times. Although these disturbances look like a successive wave motion, they are independent disturbances which passed in succession, traveling at different velocities. Each direction of these four disturbances is schematically shown in Fig. 4. Since we used four oblique beams, we can determine the azimuth angle of disturbance traveling with an error of 22.5°.

3.2. *Non-traveling disturbances*

Next we discuss the type-B disturbances. Figure 5 shows the time variation of the height z_L at which the electron density is 6×10^4 cm^{-3}, obtained by the multiple beam observation during the night of 20–21 January 1989. The height z_L corresponds to the minimum virtual height ($h'F$) of the F-layer. During this night, three disturbances in the F-region electron density were observed (REDDY *et al.*, 1990). The decrease of the height z_L at around 0120 LT began almost simultaneously in all the oblique beams, which implies that this disturbance was not traveling and its horizontal scale was larger than the distance between the oblique beams (200–300 km).

There is a possibility that the travel speed of the disturbance was so large that we could not detect exactly the phase difference between the oblique beam

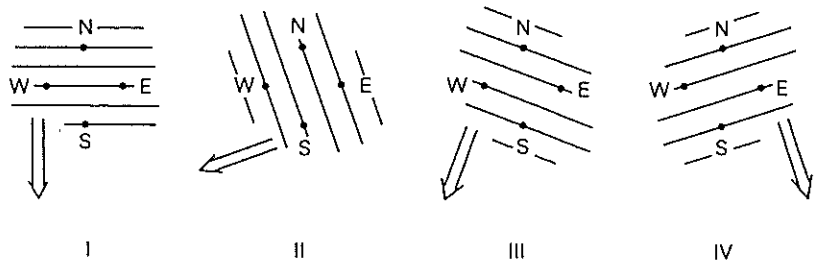

Fig. 4. Travel directions of the disturbances I, II, III and IV shown in Fig. 3. It is found that the disturbance-I came almost directly from the north, II from the east north-east, III from the north north-east and IV from the north north-west.

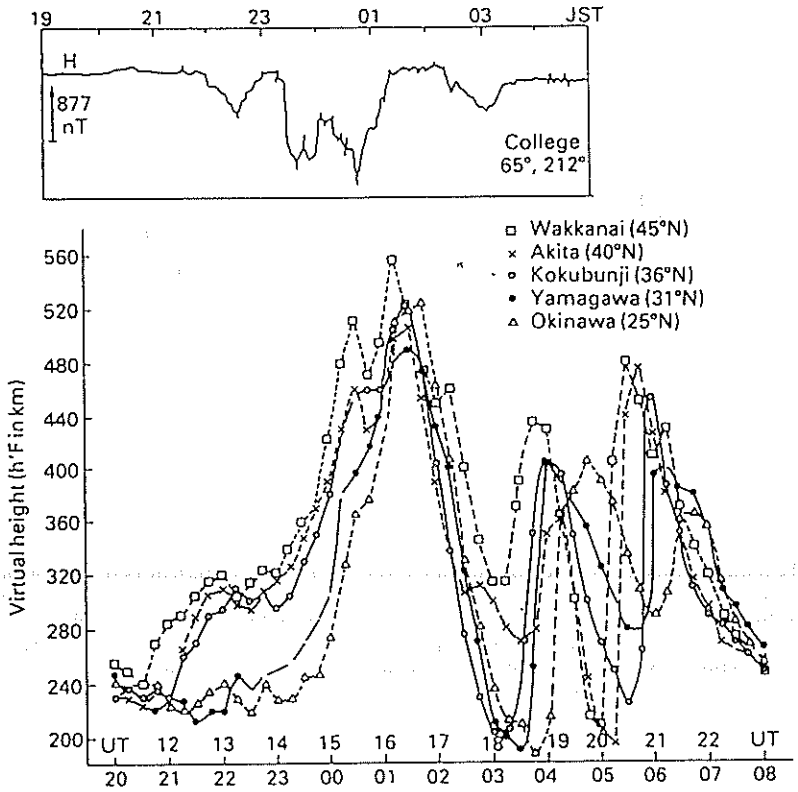

Fig. 6. Temporal variations of $h'F$ at Wakkanai (35°N, 206°), Akita (30°N, 206°), Kokubunji (26°N, 206°), Yamagawa (20°N, 198°) and Okinawa (15°N, 196°) and the H-component of the geomagnetic field at College (65°N, 212°) during the same period as Fig. 5.

signals. However, by analysing the ionograms at five ionospheric stations in Japan and the magnetogram at the auroral region together with the MU radar data, we can conclude that such a very fast traveling disturbance did not occur. Figure 6 shows the time variation of $h'F$ at Wakkanai (35°N, 206°), Akita (30°N, 206°), Kokubunji (26°N, 206°), Yamagawa (20°N, 198°) and Okinawa (15°N, 196°) and the H-component at College (65°N, 212°) during the same period as shown in Fig. 5. On the one hand, every $h'F$ value obtained at five stations had peaks at around 0120 LT which is at approximately the same time when we observed the maximum of z_l with the MU radar. This means that this disturbance had a horizontal scale much larger than the range of the MU radar observation and emerged simultaneously over a large spatial area. On the other hand, the H-component at College indicates that an intense substorm began at around 2320 LT and ended at around 0120 LT. It should be noted that the decrease of the height z_l in the MU radar data began at around 0120 LT when the substorm had just ended. This decrease of z_l may correspond to the disappearance of the eastward electric field associated with the substorm. From these features, it is confirmed that the disturbance occurring at around 0120 LT in Fig. 6 was the type-B disturbance which was not traveling and emerged simultaneously over a wide spatial area.

The height z_l measured by the MU radar data increased at 0500–0530 LT. We find that this increase of the height z_l was not associated with a type-B disturbance, but with a type-A disturbance which traveled almost directly from north to south with a horizontal speed of about 250 m/s.

4. CHARACTERISTICS OF HORIZONTAL TRAVELING DISTURBANCES

We examined 47 cases of mid-latitude, horizontal traveling ionospheric disturbances, that is, type-A, detected by the MU radar multiple beam observations. The 560-h data set of IS power profile

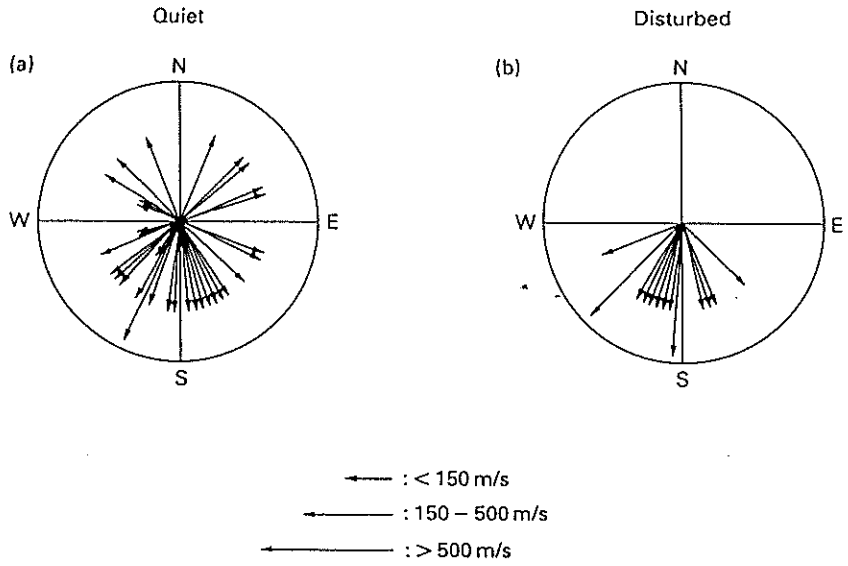

Fig. 7. The horizontal velocity of propagation of ionospheric *F*-region disturbances occurring on (a) quiet days (33 cases) and (b) disturbed days (14 cases). The arrows in these figures point in the direction of travel of these disturbances. The length of the arrow signifies the speed of these traveling disturbances. Velocities are estimated from the time variations of *F*2 peak altitudes in the four oblique beams. The traveling direction is determined with an error of 22.5° azimuth angle, so that we cannot distinguish a traveling direction from the north from that from the north north-west.

measurements with multiple beams is now available for this study. In total, there were 440 h of data on quiet days and 120 h on disturbed days. A disturbed day is defined here as a day where the maximum $K_p \geq 5$. Figure 7a shows the horizontal velocity vectors of ionospheric *F*-region disturbances occurring on quiet days (33 cases), while Fig. 7b indicates the results on disturbed days (14 cases). The velocities are estimated on the basis of time variations of *F*2 peak altitudes in the four oblique beams. The traveling directions are determined with an error of 22.5°. The speeds are classified into three levels: below 150, 150–500 and over 500 m/s.

We find that the disturbances travel primarily southward (equatorward) on disturbed days, while no preferred direction is observed on quiet days. These features suggest that polar region ionospheric disturbances associated with geomagnetic activity propagate equatorwards to mid-latitudes on disturbed days. These disturbances seem to have the same source as the disturbance observed at 0500–0530 LT on 21 January 1989 (a disturbed day), as shown in Fig. 5. We have not found wavy structures in the 47 cases examined here. It should be noted that we observed one case of a wavy structure in February 1986 (OLIVER *et al.*, 1988).

5. CONCLUDING REMARKS

The pulse-to-pulse beam steerability of the MU radar enables us to observe multiple beam positions simultaneously. This observation technique is a valuable feature of the MU radar IS observations. We use power profile measurements with a 512-μs pulse, which provides a signal-to-noise ratio sufficiently greater than unity at around the *F*2 peak altitude. Therefore, we can detect the actual difference between signal powers in different beams and investigate ionospheric disturbances in the *F*-region.

We have described two types of ionospheric disturbances, type-A and type-B, based on the data obtained by the multiple beam observations with the MU radar. Type-A disturbances are characterized by non-zero phase differences between signals detected in different beams, and are traveling disturbances. Type-B disturbances, characterized by zero phase differences between signals detected in the different beams, are generally non-propagating disturbances.

In order to investigate the characteristics of the mid-latitude ionospheric *F*-region disturbances, we examined 47 cases of ionospheric disturbances found in the data of multiple beam IS observations carried out with the MU radar for 560 h. The disturbances

travel primarily southward (equatorward) in disturbed conditions, while they have no preferred direction in quiet conditions. It is a characteristic feature that the disturbances are not wave-like but isolated events.

In this paper we have illustrated the advantage of MU radar multiple beam observations. Detailed scientific results obtained by this technique will be described in subsequent papers. The technique will be used in the near future for the study of medium-scale atmospheric gravity waves propagating in the ionosphere (e.g. HUNSUCKER, 1982).

Acknowledgements—The MU radar belongs to, and is operated by, the Radio Atmospheric Science Center of Kyoto University. The ionograms used in this study were obtained from the World Data Center C2 for Ionosphere, Communications Research Laboratory. The magnetogram used in this study was obtained from the World Data Center C2 for Geomagnetism, Faculty of Science, Kyoto University.

REFERENCES

FUKAO S., SATO T., TSUDA T., KATO S., WAKASUGI K. and MAKIHARA T. 1985a The MU radar with an active phased array system. 1. Antenna and power amplifiers. *Radio Sci.* 20, 1155.

FUKAO S., TSUDA T., SATO T., KATO S., WAKASUGI K. and MAKIHARA T. 1985b The MU radar with an active phased array system. 2. In-house equipment. *Radio Sci.* 20, 1169.

HUNSUCKER R. D. 1982 Atmospheric gravity waves generated in the high-latitude ionosphere: a review. *Rev. Geophys.* 20, 293.

OLIVER W. L., FUKAO S., SATO T., TSUDA T., KATO S., KIMURA I., ITO A., SARYO T. and ARAKI T. 1988 Ionospheric incoherent scatter measurements with the middle and upper atmosphere radar: observations during the large magnetic storm of February 6-8, 1986. *J. geophys. Res.* 93, 14649.

REDDY C. A., FUKAO S., TAKAMI T., YAMAMOTO M., TSUDA T., NAKAMURA T. and KATO S. 1990 A MU radar-based study of mid-latitude *F*-region response to a geomagnetic disturbance. *J. geophys. Res.* 95, 21077.

SARYO T., TAKEDA M., ARAKI T., SATO T., TSUDA T., FUKAO S. and KATO S. 1989 A midday bite-out event of the *F*2-layer observed by the MU radar. *J. Geomag. Geoelectr.* 41, 727.

SATO T., ITO A., OLIVER W. L., FUKAO S., TSUDA T., KATO S. and KIMURA I. 1989 Ionospheric incoherent scatter measurements with the middle and upper atmosphere radar: techniques and capability. *Radio Sci.* 24, 85.